evaporation from the hydrogel. This allows the hydrogel to work for a longer period of time with a high viability in the microchip than in an open system such as the microplate (Figs. 6 and 7). As a result of these features of the hydrogel and devices, the necessary substances and structure are provided to make it possible to keep the cells alive in the hydrogel. The microchip used in our research was fabricated on glass substrates, which are gas-impermeable materials; this is in contrast to another major chip material, poly (dimethylsiloxane) (PDMS), which is gas-permeable. Thus, for the microchip, gas transportation and exchange occur only through the microchannels and are at relatively lower levels in comparison with those in the microplate. The high long-term viability of cells in the microchip hydrogel (Figs. 5–7) implies that the hydrogel cannot only sustain the cells even under restricted conditions with a relatively low level of gas exchange but also create a static condition for cell sustainment in the microchip similar to that in bulk. In addition, the MPC units in the hydrogel created either micro- or nanoscale non-adhesive regions surrounding the cells; this caused single cells to be passively attached and thus unable to spread and flatten. Consequently, the cells in the hydrogel exhibited a round geometry, which inhibited the cell growth. The cells maintained a state with very low consumption in the confined biocompatible microscale spaces during the preservation. Therefore, the PMBV/PVA hydrogel provides a beneficial cytocompatible microenvironment that not only enables cell survival over a period of days and weeks but also significantly restrains cell growth. Nevertheless, the mechanism is still complicated and diverse; we believe that further investigation from the perspective of cell biology is necessary for future studies and will greatly help in clarifying the mechanism.

3.3. Cell cytotoxicity assays

Cell cytotoxicity assays, as examples of cell-based assays, were performed with the encapsulated L929 cells to compare the cell functions in the bulk and miniaturized hydrogels. Methanol and $CoCl_2$ solutions were used as toxins. While methanol is a strong cytotoxic agent at high concentrations, $CoCl_2$ is a non- or low cytotoxic agent according to literature [32]. Therefore, a $CoCl_2$ solution of high concentration (50 mM) and methanol solutions of low (7%, v/v) and high concentrations (70%, v/v), were prepared in 1× PBS for toxin exposure experiments. The 1× PBS solution was used as a toxin-free control. The cytotoxic sensitivity of cells in the miniaturized hydrogel (initial density: 1.0×10^6 mL^{-1} on fourth day after encapsulation) was compared with that of cells in the bulk hydrogel (initial density: 1.0×10^6 mL^{-1} on fourth day after encapsulation) according to protocols and experimental conditions similar to those described in Section 2. As shown in Fig. 8, for both hydrogels, the cytotoxicity responses of cells against toxins as expressed in the percentage of dead cells were in accordance with the cytotoxicity of the toxins; exposures to non-cytotoxic or low cytotoxic solutions (50 mM $CoCl_2$ and 7% (v/v) methanol) resulted in very low percentages of dead cells, while cell deaths of 100% were observed in exposures to the strong cytotoxic solution (70% (v/v) methanol). This indicates that cells in both hydrogel formats exhibited high cytotoxic sensitivity to different toxins with different cytotoxicities. Most importantly, for each toxin solution, the cytotoxicity response of cells in the miniaturized hydrogel was not only similar to that of cells in the bulk hydrogel but also to that of cells cultured in a medium (Fig. 8). This reveals that after encapsulation for 4 days, cells in the miniaturized hydrogel maintained a high degree of correlation in cytotoxic sensitivity with the cells in the bulk hydrogel and in the routine medium culture.

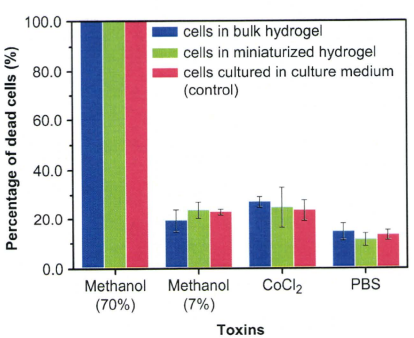

Fig. 8. Cytotoxic sensitivities of L929 cells (initial density = 1×10^6 mL^{-1}) after encapsulation for 4 days in bulk PMBV/PVA hydrogel formed in 96-well microplate and in miniaturized PMBV/PVA hydrogel formed in microchip, compared with cytotoxic sensitivity of L929 cells routinely cultured in cell culture medium (DMEM) in 96-well microplate for 2 days with approximate density of 1×10^6 mL^{-1}. The samples were directly exposed to a strong cytotoxic solution, 70% (v/v) methanol, non-cytotoxic (or low cytotoxic) solutions, 7% (v/v) methanol and 50 mM $CoCl_2$, and a toxin-free control, PBS solution. Data are expressed as mean ± SD, $n > 3$.

4. Conclusions

The performances of PMBV/PVA hydrogels formed in bulk in a 96-well microplate and in a miniaturized format in a glass microchip were compared in terms of hydrogel formation, cell encapsulation, long-term cell viability, and cell cytotoxicity. The results showed that even without an additional culture medium support, the PMBV/PVA hydrogel exhibited a uniform long-term performance in cell sustainability and cell-based assays in both bulk and miniaturized formats. The PMBV/PVA hydrogel not only provides a beneficial cytocompatible microenvironment that enables long-term cell survival but also creates a static condition for cell sustainment in the microchip similar to that in bulk. The results of this research are important and useful for the application of PMBV/PVA hydrogel system as a flexible, long-term, three-dimensional, living cell-based tool in cell-based applications on bulk to microscale levels.

Acknowledgment

This work was partially supported by a Grant-in-Aid for the Japan Society for the Promotion of Science (JSPS) Fellows (No. 19-07374).

Appendix

Figures with essential color discrimination. Many of the figures in this article are difficult to interpret in black and white. The full color images can be found in the on-line version, at doi:10.1016/j.biomaterials.2010.07.106.

References

[1] Nicodemus GD, Bryant SJ. Cell encapsulation in biodegradable hydrogels for tissue engineering applications. Tissue Eng Part B Rev 2008;14:149–65.
[2] Drury JL, Mooney DJ. Hydrogels for tissue engineering: scaffold design variables and applications. Biomaterials 2003;24:4337–51.
[3] Cushing MC, Anseth KS. Hydrogel cell cultures. Science 2007;316:1133–4.
[4] Siegel RA, Gu YD, Lei M, Baldi A, Nuxoll EE, Ziaie B. Hard and soft micro- and nanofabrication: an integrated approach to hydrogel-based biosensing and drug delivery. J Control Release 2010;141:303–13.
[5] Liu ZB, Zhang Y, Yu JJ, Mak AFT, Li Y, Yang M. A microfluidic chip with poly (ethylene glycol) hydrogel microarray on nanoporous alumina membrane for cell patterning and drug testing. Sens Actuators B Chem 2010;143:776–83.

[6] Ling Y, Rubin J, Deng Y, Huang C, Demirci U, Karp JM, et al. A cell-laden microfluidic hydrogel. Lab Chip 2007;7:756–62.
[7] Konno T, Ishihara K. Temporal and spatially controllable cell encapsulation using a water-soluble phospholipid polymer with phenylboronic acid moiety. Biomaterials 2007;28:1770–7.
[8] Xu Y, Sato K, Mawatari K, Konno T, Jang K, Ishihara K, et al. A microfluidic hydrogel capable of cell preservation without perfusion culture under cell-based assay conditions. Adv Mater 2010;22:3017–21.
[9] Whitesides GM. The origins and the future of microfluidics. Nature 2006;442:368–73.
[10] El-Ali J, Sorger PK, Jensen KF. Cells on chips. Nature 2006;442:403–11.
[11] Kane RS, Takayama S, Ostuni E, Ingber DE, Whitesides GM. Patterning proteins and cells using soft lithography. Biomaterials 1999;20:2363–76.
[12] Jang K, Sato K, Igawa K, Chung UI, Kitamori T. Development of an osteoblast-based 3D continuous-perfusion microfluidic system for drug screening. Anal Bioanal Chem 2008;390:825–32.
[13] Tanaka Y, Kikukawa Y, Sato K, Sugh Y, Kitamori T. Culture and leukocyte adhesion assay of human arterial endothelial cells in a glass microchip. Anal Sci 2007;23:261–6.
[14] Ishihara K, Ueda T, Nakabayashi N. Preparation of phospholipid polymers and their properties as polymer hydrogel membranes. Polym J 1990;22:355–60.
[15] Lewis AL. Phosphorylcholine-based polymers and their use in the prevention of biofouling. Colloids Surf B Biointerfaces 2000;18:261–75.
[16] Feng W, Brash JL, Zhu SP. Non-biofouling materials prepared by atom transfer radical polymerization grafting of 2-methacryloloxyethyl phosphorylcholine: separate effects of graft density and chain length on protein repulsion. Biomaterials 2006;27:847–55.
[17] Ishihara K, Nomura H, Mihara T, Kurita K, Iwasaki Y, Nakabayashi N. Why do phospholipid polymers reduce protein adsorption? J Biomed Mater Res 1998;39:323–30.
[18] Xu Y, Takai M, Ishihara K. Suppression of protein adsorption on a charged phospholipid polymer interface. Biomacromolecules 2009;10:267–74.
[19] McLaughlin CR, Acosta MC, Luna C, Liu WG, Belmonte C, Griffith M, et al. Regeneration of functional nerves within full thickness collagen-phosphorylcholine corneal substitute implants in guinea pigs. Biomaterials 2010;31:2770–8.
[20] Iwasaki Y, Ishihara K. Phosphorylcholine-containing polymers for biomedical applications. Anal Bioanal Chem 2005;381:534–46.
[21] Xu Y, Takai M, Konno T, Ishihara K. Microfluidic flow control on charged phospholipid polymer interface. Lab Chip 2007;7:199–206.
[22] Xu Y, Takai M, Ishihara K. Phospholipid polymer biointerfaces for lab-on-a-chip devices. Ann Biomed Eng 2010;38:1938–53.
[23] Xu Y, Takai M, Ishihara K. Protein adsorption and cell adhesion on cationic, neutral, and anionic 2-methacryloyloxyethyl phosphorylcholine copolymer surfaces. Biomaterials 2009;30:4930–8.
[24] Takahashi K, Mawatari K, Sugii Y, Hibara A, Kitamori T. Development of a micro droplet collider; the liquid–liquid system utilizing the spatial-temporal localized energy. Microfluid Nanofluid. doi:10.1007/s10404-010-0622-3.
[25] Iwasaki Y, Nakagawa C, Ohtomi M, Ishihara K, Akiyoshi K. Novel biodegradable polyphosphate cross-linker for making biocompatible hydrogel. Biomacromolecules 2004;5:1110–5.
[26] Wachiralarpphaithoon C, Iwasaki Y, Akiyoshi K. Enzyme-degradable phosphorylcholine porous hydrogels cross-linked with polyphosphoesters for cell matrices. Biomaterials 2007;28:984–93.
[27] Liu WG, Deng C, McLaughlin CR, Fagerholm P, Lagali NS, Heyne B, et al. Collagen-phosphorylcholine interpenetrating network hydrogels as corneal substitutes. Biomaterials 2009;30:1551–9.
[28] Goda T, Konno T, Takai M, Moro T, Ishihara K. Biomimetic phosphorylcholine polymer grafting from polydimethylsiloxane surface using photo-induced polymerization. Biomaterials 2006;27:5151–60.
[29] Ye SH, Watanabe J, Takai M, Iwasaki Y, Ishihara K. High functional hollow fiber membrane modified with phospholipid polymers for a liver assist bioreactor. Biomaterials 2006;27:1955–62.
[30] Iwasaki Y, Sawada S, Ishihara K, Khang G, Lee HB. Reduction of surface-induced inflammatory reaction on PLGA/MPC polymer blend. Biomaterials 2002;23:3897–903.
[31] Sawada S, Sakaki S, Iwasaki Y, Nakabayashi N, Ishihara K. Suppression of the inflammatory response from adherent cells on phospholipid polymers. J Biomed Mater Res A 2003;64A:411–6.
[32] Wang Z, Kim MC, Marquez M, Thorsen T. High-density microfluidic arrays for cell cytotoxicity analysis. Lab Chip 2007;7:740–5.

Colloids and Surfaces B: Biointerfaces 79 (2010) 357–364

Contents lists available at ScienceDirect

Colloids and Surfaces B: Biointerfaces

journal homepage: www.elsevier.com/locate/colsurfb

Simple surface modification of a titanium alloy with silanated zwitterionic phosphorylcholine or sulfobetaine modifiers to reduce thrombogenicity

Sang-Ho Ye[a,b], Carl A. Johnson Jr.[a,c], Joshua R. Woolley[a,c], Hironobu Murata[a,c], Lara J. Gamble[e], Kazuhiko Ishihara[f], William R. Wagner[a,b,c,d,*]

[a] McGowan Institute for Regenerative Medicine, University of Pittsburgh, Pittsburgh, PA 15219, USA
[b] Department of Surgery, University of Pittsburgh, Pittsburgh, PA 15219, USA
[c] Department of Bioengineering, University of Pittsburgh, Pittsburgh, PA 15219, USA
[d] Department of Chemical Engineering, University of Pittsburgh, Pittsburgh, PA 15219, USA
[e] Department of Bioengineering and NESAC/BIO, University of Washington, Seattle, WA 98195, USA
[f] Department of Materials Engineering, School of Engineering, The University of Tokyo, 7-3-1, Hongo, Bunkyo-ku, Tokyo 113-8656, Japan

ARTICLE INFO

Article history:
Received 16 March 2010
Received in revised form 16 April 2010
Accepted 19 April 2010
Available online 24 April 2010

Keywords:
Surface modification
Phosphorylcholine
Sulfobetaine
Blood compatibility
Cardiovascular devices

ABSTRACT

Thrombosis and thromboembolism remain problematic for a large number of blood contacting medical devices and limit broader application of some technologies due to this surface bioincompatibility. In this study we focused on the covalent attachment of zwitterionic phosphorylcholine (PC) or sulfobetaine (SB) moieties onto a $TiAl_6V_4$ surface with a single step modification method to obtain a stable blood compatible interface. Silanated PC or SB modifiers (PCSi or SBSi) which contain an alkoxy silane group and either PC or SB groups were prepared respectively from trimethoxysilane and 2-methacryloyloxyethyl phosphorylcholine (MPC) or *N*-(3-sulfopropyl)-*N*-(methacryloxyethyl)-*N*,*N*-dimethylammonium betaine (SMDAB) monomers by a hydrosilylation reaction. A cleaned and oxidized $TiAl_6V_4$ surface was then modified with the PCSi or SBSi modifiers by a simple surface silanization reaction. The surface was assessed with X-ray photoelectron spectroscopy (XPS), attenuated total reflection-Fourier transform infrared spectroscopy (ATR-FTIR) and contact angle goniometry. Platelet deposition and bulk phase activation were evaluated following contact with anticoagulated ovine blood. XPS results verified successful modification of the PCSi or SBSi modifiers onto $TiAl_6V_4$ based on increases in surface phosphorous or sulfur respectively. Surface contact angles in water decreased with the addition of hydrophilic PC or SB moieties. Both the PCSi and SBSi modified $TiAl_6V_4$ surfaces showed decreased platelet deposition and bulk phase platelet activation compared to unmodified $TiAl_6V_4$ and control surfaces. This single step modification with PCSi or SBSi modifiers offers promise for improving the surface hemocompatibility of $TiAl_6V_4$ and is attractive for its ease of application to geometrically complex metallic blood contacting devices.

1. Introduction

Platelet deposition still occurs on the metallic surfaces utilized in cardiovascular applications such as vascular stents, heart valves, and ventricular assist devices (VADs). As a result, patients implanted with these devices often require chronic anticoagulation or anti-platelet therapy to reduce the risks of thrombosis and thromboembolism. Unfortunately, this pharmacologic therapy comes with an increased risk of bleeding which can result in significant morbidity and mortality [1–5]. Enhancing the thromboresistance of metallic blood contacting surfaces could thus lead to more widespread application of cardiovascular devices with lower complication risks and potentially permit the development of new areas for device application.

To enhance the thromboresistance of VADs in particular, several types of coatings such as titanium nitride (TiN), diamond-like carbon (DLC), 2-methacryloyloxyethyl phosphorylcholine (MPC) polymer, and heparin coatings have been applied to metallic blood contacting surfaces [5]. MPC-based coatings, are notable in that the biomimetic and zwitterionic phosphorylcholine (PC) group-bearing polymers have demonstrated attractive levels of blood compatibility by inhibition of protein adsorption, platelet adhesion and platelet activation on modified surfaces [6–11] and they have been applied onto a variety of metallic surfaces such as vascular stents and VADs [12–15].

In a previous study assessing the preclinical biocompatibility of VAD coatings [15], a physically adsorbed MPC copolymer coating showed superior performance to a DLC coating, a more common

* Corresponding author at: McGowan Institute for Regenerative Medicine, 450 Technology Dr., Suite 300, Pittsburgh, PA 15219, USA. Tel.: +1 412 624 5324; fax: +1 412 624 5363.
E-mail address: wagnerwr@upmc.edu (W.R. Wagner).

0927-7765/$ – see front matter © 2010 Elsevier B.V. All rights reserved.
doi:10.1016/j.colsurfb.2010.04.018

coating for VADs. While DLC coatings have also demonstrated good hemocompatibility and durability independently of comparative studies with MPC, they also carry the risk of microcrack formation [16]. Unlike heparin coated surfaces, MPC copolymer coatings have not been shown to present a potential risk for heparin-induced thrombocytopenia and should be less susceptible to degradative enzymatic process that can act on heparin [17–19]. However physically adsorbed PC group-bearing polymer coatings are not as stable as DLC coatings and the concern of surface stability in long-term applications may offset its perceived advantages. MPC coatings that are covalently linked onto metallic surfaces would thus be more attractive to ensure sustained non-thrombotic properties in long-term cardiovascular applications [13,16].

Along these lines, we have recently demonstrated that a PC group-bearing polymer could be covalently bound to a titanium alloy ($TiAl_6V_4$) surface by a condensation reaction or with plasma initiated graft polymerization after the $TiAl_6V_4$ surface was treated with a functional silane coupling agent [20,21]. However, the required pre-modification steps for these reactions may have resulted in diminished control of the uniformity and coverage of the PC groups on the modified surface. A simplified surface modification technique would be attractive as it could potentially result in better control of the coating process and increase the ease and reproducibility of the coating process for bulk manufacturing as well as reduce the amount of MPC necessary for coating and thereby reduce the overall cost of the coating process.

The aim of our study was to develop a surface modification strategy to obtain a stable blood compatible interface on a $TiAl_6V_4$ surface. This surface has relevance for a number of cardiovascular devices, particularly in the rotary blood pump field where there is interest in extending this type of device therapy to the pediatric population [22]. In the present study, we focused on developing a simple modification method to covalently attach hemocompatible moieties onto a $TiAl_6V_4$ surface in a process that would be amenable to complex surfaces such as one would encounter in a rotary blood pump. For this, we prepared a silanated PC modifier (PCSi) which contains an alkoxy silane and PC groups to modify a clinically relevant $TiAl_6V_4$ surface in a single step. Additionally, in an effort with similar objectives, a silanated sulfobetaine (SB) modifier (SBSi) was also prepared. Surfaces modified with SB group-bearing polymers with zwitterionic side groups [$-N^+(CH_2)_nSO_3^-$] have also exhibited anti-bioadherent properties and non-thrombogenicity due to the ability of the surface to resist protein adsorption and platelet adhesion similar to PC group modified surfaces [23–27]. The modification effect of PCSi and SBSi modifiers on a $TiAl_6V_4$ surface was characterized and the blood compatibility of the modified surfaces was assessed in terms of platelet adhesion and activation following acute blood contact in vitro.

2. Materials and methods

2.1. Materials

Titanium alloy ($TiAl_6V_4$) was purchased (California Metal & Supply Inc., Gardena, CA) and polished with 3.0, 1.0, 0.25, and 0.1 μm diamond pastes (Electron Microscopy Sciences, Washington, PA). The polishing methodology utilized with increasingly fine pastes was matched to that employed for rotary blood pumps under development by Launchpoint Technologies (Goleta, CA). The MPC was obtained from NOF Corporation (Tokyo, Japan), and synthesized by the same method described in a previous report [6]. *N*-(3-sulfopropyl)-*N*-(methacryloxyethyl)-*N*,*N*-dimethylammonium betaine (SMDAB), trimethoxy silane (TMSi) and platinum 10 wt% on activated carbon (Pt/C) were purchased from Sigma–Aldrich (St. Louis, MO).

2.2. Synthesis of silanated zwitterionic modifier

Silanated zwitterionic surface modifiers (PCSi or SBSi) were prepared from TMSi and either MPC or SMDAB monomers by a hydrosilylation reaction. A round bottom flask equipped with magnetic stirrer was charged with anhydrous MeOH (10 mL), and MPC or SMDAB monomer (1 mmol) was dissolved under Ar gas for 30 min. TMSi (10 mmol) was then added in excess and Pt/C (0.1 g) was added as a catalyst followed by flushing with Ar gas for 10 min and sealing of the flask. The mixture was reacted at 40 °C for 24 h in an oil bath. Unreacted TMSi monomer and solvent were removed by a rotary evaporator at 40 °C under reduced pressure. After evaporation, anhydrous MeOH was added and the product filtered with a 25 mm syringe filter (poly(tetrafluoroethylene) (PTFE), 0.45 μm, Corning Inc., Corning, NY) to remove the Pt/C. MeOH was removed again by rotary evaporation. The brown, oil-like reaction product was stored in refrigerator at 4 °C after sealing the container to exclude moisture (Fig. 1). The chemical structures of the silanated PC and SB (PCSi and SBSi) were confirmed with ^{1}H NMR (300 MHz, Bruker Biospin Co., Billerica, MA).

2.3. Surface modification with the silanated MPCSi and SBSi

$TiAl_6V_4$ was polished and cleaned ultrasonically three times for 5 min each with ethanol and acetone after samples were cut to a predetermined size (1 cm × 2.5 cm) from a $TiAl_6V_4$ sheet. Titanium

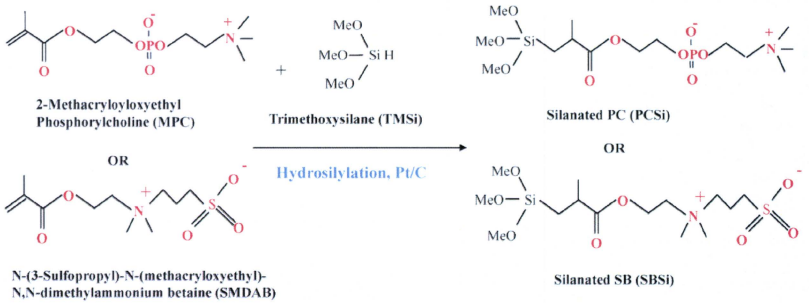

Fig. 1. Synthetic scheme for zwitterionic surface modifiers (PCSi or SBSi).

surfaces were passivated with a 35% nitric acid solution for 1 h and rinsed with distilled water for 24 h. Then, silanized titanium surfaces with the PCSi or SBSi were prepared by a hydrous liquid phase deposition method. The synthesized PCSi or SBSi was diluted at 3% concentration in MeOH and stirred for 30 min after adding the amount of necessary distilled water and HCl (0.05 M) to hydrolyze the methoxy groups of the PCSi or SBSi modifiers under acidic conditions (pH 4–5). Then the $TiAl_6V_4$ sample was immersed in the activated PCSi or SBSi solution and stirred for 30 min to adsorb the activated PCSi or SBSi on the titanium surface via weak hydrogen bonding. After that, the sample surfaces were dried in an oven for 1 h at 110 °C to silanize the surfaces with the PCSi or SBSi through covalent bonding. Samples treated in this manner were referred to as Ti-PCSi or Ti-SBSi. TMSi modified $TiAl_6V_4$ samples (Ti-TMSi) were also prepared by the same silanization reaction as a control. The modified samples were rinsed by stirring in deionized water for 24 h before using.

2.4. Surface characterization

The surface composition of the modified and unmodified $TiAl_6V_4$ samples was analyzed by X-ray photoelectron spectroscopy (XPS) using a Surface Science Instruments S-probe spectrometer at the University of Washington (Seattle, WA). The surface composition on a given sample was averaged from three composition spots. The mean value for three different samples was determined. The modified $TiAl_6V_4$ surfaces were also analyzed with an attenuated total reflection-Fourier transform infrared spectroscopy (ATR-FTIR, Shimadzu, Columbia, MD). The spectra were collected with 1024 scans at a resolution of 4 cm^{-1}. The static contact angle of water on the surfaces of unmodified and modified titanium samples was measured at room temperature using a contact angle goniometer (VCA optima, AST Product Inc., Billerica, MA) by placing 1 μL of distilled water on the surfaces. The contact angle was also measured after 4 weeks in the surface modified samples that underwent continuous stirring under deionized water to test the long-term stability of the surface modification. The $TiAl_6V_4$ surfaces were stained with rhodamine 6G (Sigma–Aldrich, St. Louis, MO) by immersing in rhodamine 6G aqueous solution (0.2 mg/mL) for 30 s, followed by washing in distilled water for 30 s and drying [28,29]. The surfaces were observed with fluorescence microscopy (ZEISS, Carl Zeiss, Inc. Thornwood, NY) and obtained images were analyzed with an Image-J program (National Institutes of Health, Washington, DC).

2.5. Surface protein adsorption

Surface protein adsorption on modified and unmodified $TiAl_6V_4$ samples was assessed by a micro-bicinchoninic acid (BCA) assay [30]. Ovine fibrinogen (Sigma–Aldrich) was prepared in phosphate buffer solution (PBS; BD Biosciences, San Jose, CA) at a concentration of 0.03 g/dL. The samples were immersed in the fibrinogen solution at 37 °C for 3 h followed by washing with 50 mL PBS. A protein analysis kit (Quantipro-Micro BCA kit, Sigma–Aldrich) based on the BCA method was used to quantify adsorbed fibrinogen. The mean value of fibrinogen adsorption from five independent samples, each measured in triplicate, was determined.

2.6. Blood collection and blood contact test

NIH guidelines for the care and use of laboratory animals were observed. Whole blood was collected from healthy ovines by jugular venipuncture using an 18 gauge 1.5″ needle after discarding the first 3 mL, and 2.7 mL was then immediately added to monovette tubes containing 0.3 mL of 0.106 M trisodium citrate (Sarstedt, Newton, NC). Whole ovine blood was also collected by jugular venipuncture directly into a syringe containing heparin (3.0 or 6.0 U/mL) after discarding the first 3 mL for blood contacting experiments. Then, modified titanium and unmodified $TiAl_6V_4$ samples were placed into Vacutainer® blood collection tubes without additives (BD Biosciences, Franklin Lakes, NJ), filled with citrate or heparinized ovine blood and incubated at 37 °C on a hematology mixer (Fisher Scientific, Pittsburgh, PA). Although some anticoagulation is necessary to perform the blood contact testing, citrate and heparin were both used to provide a comparison between stronger (citrate) and weaker (heparin) inhibitors of platelet deposition.

2.7. Scanning electron microscopy of platelet adhesion and morphology

After contact with citrated or heparinized ovine blood, surfaces were rinsed with PBS and immersed in a 2.5% glutaraldehyde solution for 2 h at 4 °C to fix the surface adherent platelets, and treated for 1 h in 1% (w/v) OsO_4. The samples were serially dehydrated with increasing ethanol solutions and sputter coated with gold/palladium. Each sample surface was observed by scanning electron microscopy (SEM; JSM-6330F, JEOL USA, Inc., Peabody, MA).

2.8. Quantification of platelet adhesion and activation

Modified and unmodified titanium samples were incubated with heparinized ovine blood for 2 h at 37 °C with continuous rocking as above. The surfaces were rinsed thoroughly after blood contact with 50 mL of PBS and immersed in 1 mL of 2% Triton X-100 solution (Sigma) for 20 min to lyse surface adherent platelets. The number of deposited platelets on each sample was then quantified by a lactate dehydrogenase (LDH) assay [31] with an LDH Cytotoxicity Detection Kit (Takara Bio, Tokyo, Japan). Calibration of spectrophotometer absorbance results to platelet numbers was accomplished using a calibration curve generated from known dilutions of ovine platelet rich plasma in the lysing solution. The

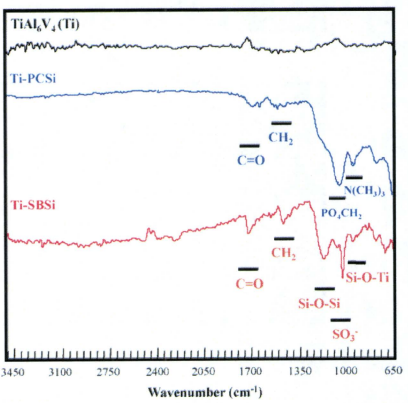

Fig. 2. Attenuated total reflectance (ATR)-FTIR spectra on the unmodified titanium ($TiAl_6V_4$ (Ti)), Ti-PCSi and Ti-SBSi.

Table 1
Atomic percentage at listed binding energy (eV) as determined by X-ray photoelectron spectroscopy.

	C 1s at 285 eV	O 1s at 532 eV	Ti 2p at 455 eV	Al 2p at 74 eV	Si 2p at 106 eV	N 1s at 403 eV	P 2p at 133 eV	S 2p at 168 eV
$TiAl_6V_4$ (Ti)	42.0 (±8.0)	41.1 (±5.2)	9.5 (±1.1)	4.3 (±3.1)	1.0 (±1.0)	1.0 (±0.5)	0.1 (±0.2)	0.0 (±0.0)
Ti-TMSi	44.8 (±12.9)	33.3 (±7.7)	2.3(±1.2)	2.7 (±1.5)	13.1 (±2.7)*	0.8 (±0.7)	0.0 (±0.0)	0.0 (±0.0)
Ti-PCSi	32.3 (±4.9)	47.4 (±3.9)	0.3 (±0.5)	0.5 (±0.8)	16.2 (±3.7)*	1.7 (±0.4)*	1.5 (±0.3)*	0.0 (±0.0)
Ti-SBSi	37.0 (±8.2)	40.3 (±6.8)	0.0 (±0.0)	1.2 (±2.1)	17.6 (±4.9)*	2.0 (±0.7)	0.0 (±0.0)	2.0 (±0.9)*

$N = 7$, ±standard deviation for Ti. $N = 3$, ±standard deviation for other samples.
* $p < 0.05$ vs. Ti surfaces.

percentage of activated ovine platelets in the bulk phase of the blood contacting the surface samples was quantified by a flow cytometric assay using fluorescein conjugated Annexin V protein [32]. Activation levels from five independent samples were averaged for each surface type after subtracting the level of activation found for tubes filled with ovine blood that were rocked in the absence of a metallic surface specimen.

2.9. Statistical analyses

Data are presented as means with standard deviation. Statistical significance between sample groups was determined using ANOVA followed by post-hoc Newman–Keuls testing of specific differences. Statistical significance was considered to exist at $p < 0.05$.

3. Results

3.1. Surface modification and characterization of the modified $TiAl_6V_4$ with silanated zwitterionic modifier PCSi or SBSi

To achieve one-step surface modification of $TiAl_6V_4$ with non-specific protein adsorption, silanated zwitterionic modifier PCSi or SBSi were synthesized by hydrosilylation between trimethoxysilane and MPC or SMDAB. The hydrosilylation in this study occurred on Si–H to alkene group in the methacryloyl group of MPC and SMDAB in the presence of a platinum catalyst. The chemical structure of the synthesized PCSi and SBSi was confirmed by ^{1}H NMR. For PCSi (in deuterated ethanol) the peaks were: δ (ppm) 1.07–1.10 ($SiCH_2CHCH_3$, 2H), 1.15–1.20 ($SiCH_2CHCH_3$, 1H),

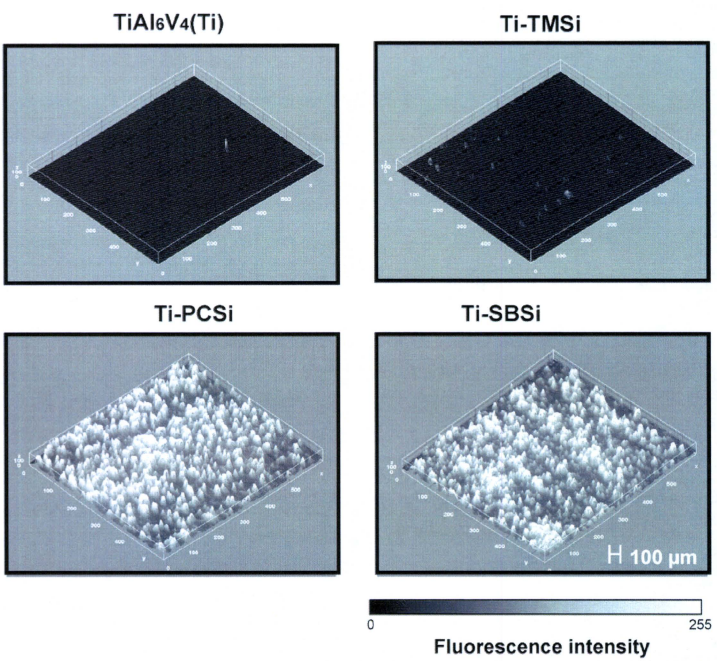

Fig. 3. Fluorescent micrograph images of unmodified $TiAl_6V_4$ (Ti), Ti-TMSi, Ti-PCSi and Ti-SBSi observed after staining with rhodamine 6G and digital image processing to create a 3D plot where the z-dimension is proportional to pixel intensity.

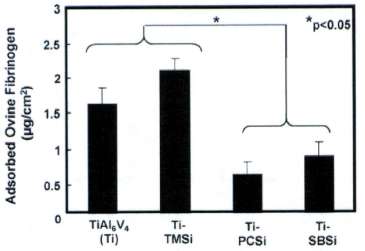

Fig. 4. Ovine fibrinogen adsorption from buffer at 37 °C for 3 h onto surfaces of control tissue culture polystyrene, unmodified and modified $TiAl_6V_4$ samples as determined by micro-BCA assay ($n = 5$).

1.90–2.11 ($SiCH_2CHCH_3$, 3H), 3.21–3.26 ($N(CH_3)_3$, 9H), 3.42–3.53 ($Si(OCH_3)_3$, 9H), 3.79–3.83 ($CH_2N(CH_3)_3$ 2H), 3.96–4.01 (OCH_2, 2H), 4.05–4.15 ($CH_2PO_4CH_2$, 4H), and for SBSi (in deuterated ethanol) the peaks were: δ (ppm) 0.92–0.94 ($SiCH_2CHCH_3$, 2H), 1.17–1.29 ($SiCH_2CHCH_3$, 3H), 1.37 ($SiCH_2CHCH_3$, 1H), 2.18–2.28 (CH_2CH_2S, 2H), 2.82–2.86 (CH_2CH_2S, 2H), 3.22–3.28 ($N(CH_3)_2$, 6H), 3.28–3.38 ($Si(OCH_3)_3$, 9H), 3.69–3.83 ($CH_2N(CH_3)_2CH_2$, 4H) and 4.54–4.60 (OCH_2, 2H).

The surface composition analyzed by XPS is also shown in Table 1. The surfaces modified with TMSi which were prepared as a control showed a decrease in Ti composition and increased Si composition in comparison with unmodified $TiAl_6V_4$ (Ti) ($p < 0.05$). The data also support the successful modification of $TiAl_6V_4$ surfaces with the PCSi or SBSi based on an increased phosphorus composition ($P = 1.5 \pm 0.2\%$) on the surface of Ti-PCSi and an increased sulfur composition ($S = 2.5 \pm 1.1\%$) on the surface of Ti-SBSi in comparison to unmodified $TiAl_6V_4$ (Ti) and Ti-TMSi ($p < 0.05$). An attenuated total reflection FTIR spectrum for each surface is shown in Fig. 2. On the surface of Ti-PCSi and SBSi, there are new absorbance peaks at 1723 cm^{-1} (C=O stretching vibration), 1480–1300 cm^{-1} (CH_2, CH_3 bending), 1250–1020 cm^{-1} (Si–O–Si asymmetric stretching vibration), 1150–1050 cm^{-1} ($PO_4CH_2^-$ stretching vibration), 1172, 1040 cm^{-1} (SO_3^- vibration), 970 cm^{-1} ($N(CH_3)_3$ vibration), 925–950 cm^{-1} (Si–O–Ti siloxane bond to titanium) [33,34].

Fluorescent micrograph images of unmodified $TiAl_6V_4$ (Ti), Ti-TMSi, Ti-MPCSi and Ti-SBSi observed after staining with rhodamine 6G and generating 3D plots of the fluorescence intensity are seen in Fig. 3. Both the PCSi modified surface (Ti-PCSi) and the Ti-SBSi stained strongly with the rhodamine and coverage was relatively uniform. Unmodified $TiAl_6V_4$ (Ti) and Ti-TMSi control surfaces did not stain positively and yielded dark images.

Table 2 shows the surface contact angle before and after surface modification. The surface contact angles significantly decreased on both the Ti-PCSi and Ti-SBSi in comparison with $TiAl_6V_4$ (Ti) and Ti-TMSi attributable to the presence of the hydrophilic PC and SB groups on the surfaces. The contact angles did not significantly change after continuous rinsing with deionized water over a 4 week period.

The amount of adsorbed ovine fibrinogen on the unmodified and modified titanium surfaces is shown in Fig. 4. Both the Ti-PCSi and Ti-SBSi showed a significant decrease in adsorbed fibrinogen relative to Ti and Ti-TMSi surfaces.

3.2. *In vitro surface blood compatibility of the modified $TiAl_6V_4$*

Electron micrographs of platelet deposition from citrated ovine blood for 3 h at 37 °C for unmodified $TiAl_6V_4$ (Ti) and modi-

Table 2
Contact angle with distilled water on the unmodified and modified titanium samples.

	$TiAl_6V_4$ (Ti)	Ti-TMSi	Ti-PCSi	Ti-SBSi	Ti-PCSi after 4 weeks of rinsing	Ti-SBSi after 4 weeks of rinsing
Contact angle (°)	53.7 (±4.1)	95.2 (±4.1)	16.4 (±3.9)*	21.8 (±5.5)*	22.9 (±3.2)*	24.9 (±4.4)*

$N = 3$, ±standard deviation.
* $p < 0.05$ vs. Ti and Ti-TMSi surfaces.

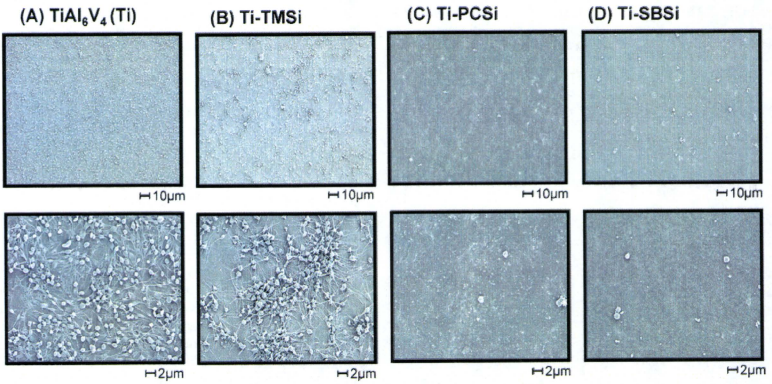

Fig. 5. Low (top row) and high (bottom row) magnification scanning electron micrographs of $TiAl_6V_4$ (Ti), Ti-TMSi, Ti-PCSi and Ti-SBSi samples after contact with fresh ovine blood (citrated) under mixing for 3 h at 37 °C.

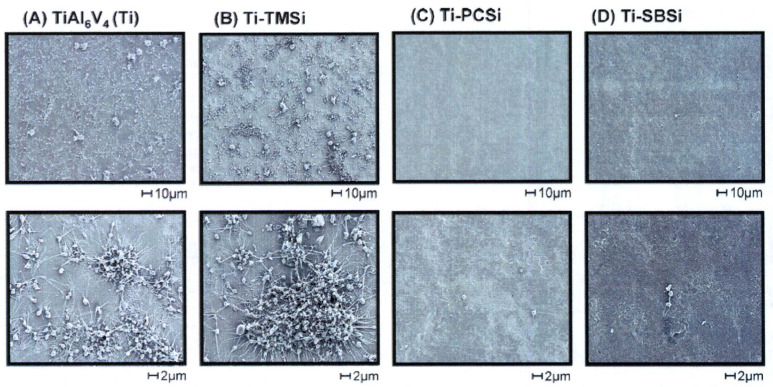

Fig. 6. Low (top row) and high (bottom row) magnification scanning electron micrographs of $TiAl_6V_4$ (Ti), Ti-TMSi, Ti-PCSi and Ti-SBSi samples after contact with fresh ovine blood (with heparin at 3 U/mL) under mixing for 2 h at 37 °C.

fied titanium samples (Ti-TMSi, Ti-PCSi and Ti-SBSi) are shown in Fig. 5. There were many adhered platelets on the unmodified Ti and Ti-TMSi surfaces and some platelet aggregation was seen. The deposited platelets exhibited an activated morphology, as demonstrated by extended pseudopodia and surface spreading. In contrast, platelet deposition was sparse on the Ti-PCSi and Ti-SBSi surfaces and those platelets found were in a discoid morphology without signs of surface activation. Platelet adhesion and morphology was also observed after contact with heparinized ovine blood (3 U/mL) for 2 h at 37 °C (Fig. 6). Platelet deposition and surface aggregation appeared to increase on the Ti and Ti-TMSi surfaces with the heparinized blood when compared to surfaces in contact with citrated blood. The marked decrease in platelet deposition on the Ti-PCSi and Ti-SBSi surfaces compared to the Ti and Ti-TMSi samples was again observed with the heparinized blood.

The number of deposited platelets as quantified by the lactate dehydrogenase (LDH) assay after heparinized ovine blood contact is shown in Fig. 7. The Ti-PCSi and Ti-SBSi modified surfaces showed large decreases in the number of deposited platelets relative to unmodified $TiAl_6V_4$ and Ti-TMSi ($p < 0.01$). However, the Ti-PCSi

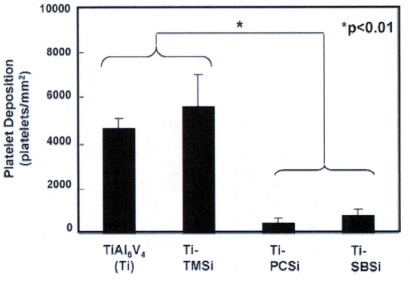

Fig. 7. Platelet deposition onto surfaces after contact with ovine blood (with heparin at 6 U/mL) for 2 h under mixing as determined by lactate dehydrogenase (LDH) assay ($n = 5$).

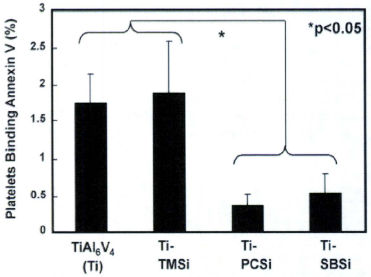

Fig. 8. Quantification of activated platelets in the bulk phase of ovine blood after surface contact under continuous rocking. Platelet activation was quantified by flow cytometric measurement of Annexin V binding onto platelets ($n = 5$). The background platelet activation level was determined from a rocked tube into which no test surface was placed. This background value was subtracted from all tests where a surface was included.

was not significantly different than the Ti-SBSi surfaces. Platelet activation in the bulk phase, as evidenced by Annexin V binding, for ovine blood after contact with the unmodified and modified titanium samples is shown in Fig. 8, where platelet activation levels following contact with Ti-PCSi and Ti-SBSi samples were significantly lower than that for unmodified $TiAl_6V_4$ (Ti) and Ti-TMSi control samples.

4. Discussion

There is increasing interest in zwitterionic moieties including carboxybetaine (CB), sulfobetaine (SB) and phosphobetaine (PC group-bearing polymer) to design biocompatible polymeric materials since surfaces modified with these moieties are less supportive of untoward cell adhesion or enzymatic activation based on their minimization of protein adsorption [35]. Kitano et al. [36–38] showed common effects of zwitterionic group-bearing polymer surfaces on the structure of surrounding water in that PC, SB or

CB groups did not disturb the hydrogen-bonding network structure of water. It was further suggested that the resistance of these surfaces to protein adsorption related to the local water structure [39].

To initiate chemical modification of a polymeric biomaterial surface, there are many approaches that have been pursued, including direct grafting with a zwitterionic group containing monomer [24,25,40–42] or the use of alkoxysilane compounds which have PC, SB or CB groups such as PCSi or SBSi as surface modifiers [43,44]. However, previous studies have required a complicated synthesis route to generate the appropriate PC or SB groups and attach these onto the surface. In this report we simply prepared PCSi and SBSi as titanium alloy surface modifiers by a hydrosilylation reaction using MPC or SMDAB. This reaction between a hydride-siloxane (Si–H) and vinyl (C=C) compounds with a catalyst such as Pt/C is relatively simple and is widely used in the silicone industry to prepare monomers, silicone-carbon compounds and crosslinkable polymers [45]. In this study, there was concern about the lower reactivity of methacrylate groups in comparison with vinyl groups [46], however the hydrosilylation of methacrylate groups was confirmed at almost 100% completion under mildly increased temperature (40 °C), provided the Si–H and catalyst were in excess and the reaction time was sufficient. The NMR analysis of synthesized PCSi and SBSi did not show any double bond peaks at 5.2–5.5 and 6.0–6.2 ppm, which would be associated with unreacted monomers. The purified PCSi and SBSi product could be collected and stored without aggregation of the siloxane compounds by keeping anhydrous conditions during the synthesis process.

West et al. [26] evaluated two copolymers containing SB or PC moieties for use as potential biocompatible coatings. They showed that both SB and PC group-bearing polymer coatings reduced cell adhesion (bacterial adhesion, human macrophages, and granulocytes) with respect to the uncoated materials, and that PC group-bearing copolymer coatings were superior to the SB-based copolymer coatings in reducing cellular adhesion. In this study, we prepared a titanium alloy surface that was modified with PC or SB groups using silanated PC or SB modifiers (PCSi or SBSi) and the modified surfaces (Ti-PCSi or Ti-SBSi) were compared in terms of fibrinogen adsorption, platelet deposition and platelet activation. Both the Ti-PCSi and Ti-SBSi surfaces experienced significantly reduced fibrinogen adsorption, platelet deposition and bulk phase platelet activation relative to unmodified Ti and Ti-TMSi control samples. Although there was a trend toward lower average values for platelet deposition, fibrinogen adsorption, and platelet activation for the Ti-PCSi relative to the Ti-SBSi, none of these differences were found to be statistically significant.

The PCSi and SBSi modified surfaces were prepared by hydrous liquid phase deposition so that the three methoxy groups of the PCSi and SBSi were changed to hydroxyl groups and the hydrolyzed PCSi and SBSi were deposited in the bulk state. The hydrolyzed modifiers had three reactive sites (hydroxyl groups) and could react with each other as well as the desired hydroxyl groups of the titanium surface. This alternative reaction by the PCSi and SBSi with tri-hydroxyl groups could result in non-uniform surfaces (bulk deposition of the PCSi and SBSi) as was seen to some extent with rhodamine staining. A relatively large variation was also observed in the SBSi composition of Ti-SBSi samples as evidenced by the XPS results (Table 1). The surface uniformity might be better controlled by changing the PCSi or SBSi modifiers concentration, silanization conditions or the modifier reactivity. A more uniform surface could be obtained by an anhydrous liquid phase deposition method where the PCSi and SBSi could deposit on the titanium surface in anhydrous toluene with a catalyst at room temperature by stirring for 24 h without hydrolysis of the methoxy groups. Toward this end we also prepared a PCSi or SBSi monolayer deposited surfaces with these surface modifiers and mono-functional silanated PCSi and SBSi modifiers from 1-chlorodimethylsilane with the same hydrosilylation reaction, and then reacted with the titanium surface to prepare a more uniform surface. The mono-functional silanated PCSi and SBSi modification on a $TiAl_6V_4$ surface also showed a significant decrease in platelet adhesion and activation compared to the control surface. However, it was difficult to prepare a highly covered monolayer with these mono-functional modifiers and the modified surfaces did not show improved performance in decreasing platelet deposition and activation relative to the bulk deposited PCSi or SBSi modified surfaces (data not shown). This may have been due to difficulty in achieving monolayer coverage with PCSi and SBSi modifiers because of imperfect monolayer availability of hydroxyl groups on the alloy substrate. In this study, we did not apply a water plasma treatment before the PCSi and SBSi modification, though we demonstrated that water plasma treatment could increase the surface reactivity of the titanium alloy in previous studies [20,21]. Better monolayer deposition may have resulted from further surface treatment, such as water plasma exposure or other chemical pretreatments, to increase hydroxyl group numbers on the surface before silanization with the PCSi and SBSi modifiers. However, the bulk deposition of PCSi or SBSi prepared under the hydrous liquid phase deposition conditions may have increased the coverage and modification density of the PC or SB groups on the surface without needing to increase the reactive hydroxyl groups on the bare titanium surface.

Previously we reported that PC group-bearing polymers could be attached onto a titanium alloy surface by immobilizing an MPC copolymer (poly(MPC-co-methacryl acid) (PMA)) or by plasma induced MPC grafting polymerization after the titanium surface was pre-modified with a functional silane coupling agent [20,21]. Those surfaces showed significant improvement over non-modified surfaces in terms of decreased platelet deposition and bulk phase platelet activation. However, those techniques required multiple steps to pre-functionalize the surface in order to immobilize or graft the PC group-bearing polymer onto the titanium surface. There was no significant difference in terms of the inhibition of platelet deposition and activation when comparing the current one-step procedure with these previous titanium surfaces modified with PC group-bearing polymers [20,21]. The simpler and equally effective surface modification method using a small silanated PC molecule (PCSi) thus is more attractive in that this coating could be applied in a direct manner under mild conditions and could be readily applied to the assembled, complex geometries of a cardiovascular device such as a rotary blood pump [47].

While in our study the SB-based surface modification did not exhibit a significantly greater biological effect than that found with PCSi, and in fact trended to less of an effect, further investigation of this surface modifier is warranted due to its cost being orders of magnitude lower than for the PC-containing modifier. Earlier studies by Bernards et al. [48] prepared nonfouling polymer brushes composed of varying mixtures of positively [$-N^+$] and negatively [$-SO_3^-$] charged monomers by surface initiated atom transfer polymerization (ATRP) on a gold-coated surface. Their results demonstrated that the polymer brush surface coating composed of oppositely charged monomers exhibited low protein adsorption. Their best nonfouling surface coating was copolymer brushes formed from a 1:1 homogeneous reaction mixture of two oppositely charged monomers. Furthermore, Zhang et al. [49] prepared a "superlow" fouling surface on glass slides by grafting SB- or CB-bearing polymers by surface initiated ATRP. Better controlled surface modification techniques such as offered by surface initiated ATRP might maximize the surface modification effect of sulfobetaine and result in further improvements in surface blood biocompatibility.

Some limitations of the current report should be noted. First, in this study, we polished a raw titanium alloy sheet by hand with

diamond pastes of 3, 1, 0.25 and 0.1 μm size. While this level of polish was utilized to mimic the materials being employed industrially for a blood pump, the roughness of the polished, unmodified titanium surface was of a scale that additional texture added from the surface modification would not likely be detectable by AFM and ellipsometry, as noted in our previous study [21]. A more complete surface modification and more extensive surface analysis would be possible if a more highly polished surface were to be employed, although this would not likely match the types of surfaces utilized with many devices being employed clinically. Second, the amount of adsorbed protein estimated by the micro-BCA method (Fig. 4) was higher than for previous reports where the zwitterionic PC or SB groups have been attached in monolayer to more idealized surfaces [27,48]. In these reports more accurate quantification methods, such as a quartz crystal microbalance (QCM) and surface plasmon resonance (SPR), were employed. In this study, the micro-BCA method was used to provide for a relatively simple comparison between unmodified and variably modified surfaces and the levels of fibrinogen adsorption measured were generally consistent with previous reports employing the micro-BCA method [10,20]. Finally, the efficacy of the generated surfaces was evaluated in an in vitro setting, with ovine blood, for a relatively limited period of blood contact. While blood mixing was present, the hemodynamic environment would not match either the high flow regimes experienced in, for instance, a rotary blood pump, nor would there be the non-ideal flow conditions that one might experience in a crevice formed by connecting metallic parts or in regions of flow recirculation behind impeller blades [47]. Next steps for surface evaluation would involve the coating of cardiovascular devices for extended blood contact under relevant hemodynamic conditions with in vitro perfusion loops, and with testing in appropriate large animal models. A challenge with such experiments is the expense of generating multiple devices for comparative testing and the maintenance of implanted animals, although such experiments are possible and have shown the potential benefits of MPC-based coatings on blood pump biocompatibility in vivo [15].

5. Conclusions

Silanated zwitterionic surface modifiers (PCSi or SBSi) were successfully prepared from trimethoxysilane and MPC or SMDAB by a hydrosilylation reaction. Non-thrombogenic interfaces were simply achieved on a $TiAl_6V_4$ surfaces by the covalent attachment of PCSi or SBSi onto the surface in a single step modification reaction. Platelet deposition and bulk phase platelet activation were significantly decreased on PCSi or SBSi modified $TiAl_6V_4$ surfaces in comparison with unmodified and trimethoxysilane modified control surfaces. This single step modification with PCSi or SBSi modifiers offers promise for improving the surface hemocompatibility of blood contacting devices utilizing $TiAl_6V_4$ and is attractive for its ease of application to potentially complex device surfaces.

Acknowledgements

This research was supported by the NSF Engineering Research Center for Revolutionizing Metallic Biomaterials (Award #0812348) and NIH contract # HHSN268200448192C. Mr. Johnson was supported by a United Negro College Fund MERCK Graduate Science Research Dissertation Fellowship. Mr. Woolley was supported by NIH training grant # T32-HL076124.

References

[1] L.R. McBride, K.S. Naunheim, A.C. Fiore, D.A. Moroney, M.T. Swartz, Ann. Thorac. Surg. 67 (1999) 1233.
[2] X. Liu, P.K. Chu, C. Ding, Mater. Sci. Eng. R 47 (2004) 49.
[3] M.A. Simon, J. Watson, J.T. Baldwin, W.R. Wagner, H.S. Borovetz, Annu. Rev. Biomed. Eng. 10 (2008) 59.
[4] C. Hansi, A. Arab, A. Rzany, I. Ahrens, C. Bode, C. Hehrlein, Catheter. Cardiovasc. Interv. 73 (2009) 488.
[5] D.C. Sin, H.L. Kei, X. Miao, Expert Rev. Med. Devices 6 (2009) 51.
[6] K. Ishihara, T. Ueda, N. Nakabayashi, Polym. J. 22 (1990) 355.
[7] K. Ishihara, Trends Polym Sci. 5 (1997) 401.
[8] A.L. Lewis, Colloids Surf. B: Biointerfaces 18 (2000) 261.
[9] K. Ishihara, Sci. Technol. Adv. Mater. 1 (2000) 131.
[10] S.H. Ye, J. Watanabe, Y. Iwasaki, K. Ishihara, Biomaterials 24 (2003) 4143.
[11] K. Ishihara, M. Takai, J. R. Soc. Interface 6 (2009) S279.
[12] D.M. Whelan, W.J. Giessen, S.C. Krabbendam, E.A. Vliet, P.D. Verdouw, P.W. Serruys, H.M.M. Beusekom, Heart 83 (2000) 338.
[13] M. Galli, L. Sommariva, F. Prati, S. Zerboni, A. Politi, R. Bonattie, S. Mameli, E. Butti, A. Pagano, G. Ferrari, Catheter. Cardiovasc. Interv. 53 (2001) 182.
[14] S. Kihara, K. Yamazaki, P. Litwak, M.V. Kameneva, H. Ushiyama, T. Tokuno, D.C. Borzelleca, M. Umezu, J. Tomioka, O. Tagusari, T. Akimoto, H. Koyanagi, H. Kurosawa, R.L. Kormos, B.P. Griffith, Artif. Organs 27 (2003) 188.
[15] T.A. Snyder, H. Tsukui, S. Kihara, T. Akimoto, K.N. Litwak, M.V. Kameneva, K. Yamazaki, W.R. Wagner, J. Biomed. Mater. Res. 81 (2007) 85.
[16] A. Shirakura, M. Nakaya, Y. Koga, H. Kodama, T. Hasebe, T. Suzuki, Thin Solid Films 494 (2006) 84.
[17] D. Cruz, R. Karlsberg, Y. Takano, M. Rosove, D. Vora, J. Tobis. Catheter. Cardiovasc. Interv. 58 (2003) 80.
[18] J.A. Bittl, Catheter. Cardiovasc. Interv. 58 (2003) 84.
[19] L. Mureebe, J. Graham, R. Bush, D. Silver, Ann. Vasc. Surg. 21 (2007) 719.
[20] S.H. Ye, C.A. Johnson Jr., J.R. Woolley, T.A. Snyder, L.J. Gamble, W.R. Wagner, J. Biomed. Mater. Res. A 91 (2009) 18.
[21] S.H. Ye, C.A. Johnson Jr., J.R. Woolley, H.I. Oh, L.J. Gamble, K. Ishihara, W.R. Wagner, Colloids Surf. B: Biointerfaces 74 (2009) 96.
[22] H.S. Borovetz, S. Badylak, J.R. Boston, C. Johnson, R. Kormos, M.V. Kameneva, M. Simaan, T.A. Snyder, H. Tsukui, W.R. Wagner, J. Woolley, J. Antaki, C. Diao, S. Vandenberghe, B. Keller, V. Morell, P. Wearden, S. Webber, J. Gardiner, C.M. Li, D. Paden, B. Paden, S. Snyder, J. Wu, G. Bearnson, J.A. Hawkins, G. Jacobs, J. Kirk, P. Khanwilkar, P.C. Kouretas, J. Long, R.E. Shaddy, Cell Transplant. 15 (Suppl. 1) (2006) 69 (review).
[23] R.E. Holmlin, X. Chen, R.G. Chapman, S. Takayama, G.M. Whitesides, Langmuir 17 (2001) 2841.
[24] Y.L. Yuan, F. Ai, J. Zhang, X.B. Zang, J. Shen, S.C. Lin, J. Biomater. Sci. Polymer Ed. 13 (2002) 1081.
[25] J. Zhang, J. Yuan, Y.L. Yuan, X.P. Zang, J. Shen, S.C. Lin, Biomaterials 24 (2003) 4223.
[26] S.L. West, J.P. Salvage, E.J. Lobb, S.P. Armes, N.C. Billingham, A.L. Lewis, G.W. Hanlon, A.W. Lloyd, Biomaterials 25 (2004) 1195.
[27] H. Kitano, A. Kawasaki, H. Kawasaki, S. Morokoshi, J. Colloid Interface Sci. 282 (2005) 340.
[28] J.H. Wang, J.D. Bartlett, A.C. Dunn, S. Small, S.L. Willis, J. Driver, A.L. Lewis, J. Microsc. 217 (2005) 216.
[29] M. Kyomoto, Y. Iwasaki, T. Moro, T. Konno, F. Miyaji, H. Kawaguchi, Y. Takatori, K. Nakamura, K. Ishihara, Biomaterials 28 (2007) 3121.
[30] P.K. Smith, R.I. Krohn, G.T. Hermanson, A.K. Mallia, F.H. Gartner, M.D. Provenzano, E.K. Fujimoto, N.M. Goeke, B.J. Olson, D.C. Klenk, Anal. Biochem. 150 (1985) 76.
[31] Y. Tamada, E.A. Kulik, Y. Ikada, Biomaterials 16 (1995) 259.
[32] C.A. Johnson Jr., T.A. Snyder, J.R. Woolley, W.R. Wagner, Artif. Organs 32 (2008) 136.
[33] Y.L. Yuan, F. Ai, X.P. Zang, W. Zhang, J. Shen, S.C. Lin, Colloids Surf. B: Biointerfaces 35 (2004) 1.
[34] J.P. Matinlinna, S. Areva, L.V.J. Lassila, P.K. Vallittu, Surf. Interface Anal. 36 (2004) 1314.
[35] H. Chen, L. Yuan, W. Song, Z. Wu, D. Li, Prog. Polym. Sci. 33 (2008) 1059.
[36] H. Kitano, K. Sudo, K. Ichikawa, M. Ide, K. Ishihara, J. Phys. Chem. B 104 (2000) 11425.
[37] H. Kitano, M. Imai, T. Mori, M. Gemmei-Ide, Y. Yokoyama, K. Ishihara, Langmuir 19 (2003) 10260.
[38] H. Kitano, S. Tada, T. Mori, K. Takaha, M. Gemmei-Ide, M. Tanaka, M. Fukuda, Y. Yokoyama, Langmuir 21 (2005) 11932.
[39] K. Ishihara, H. Nomura, T. Mihara, K. Kurita, Y. Iwasaki, N. Nakabayashi, J. Biomed. Mater. Res. 39 (1998) 323.
[40] Z.K. Xu, Q.W. Dai, J. Wu, X.J. Huang, Q. Yang, Langmuir 20 (2004) 1481.
[41] X.J. Huang, Z.K. Xu, L.S. Wan, Z.G. Wang, J.L. Wang, Langmuir 21 (2005) 2941.
[42] P. Chevalllier, R. Janvier, D. Mantovani, G. Laroche, Macromol. Biosci. 5 (2005) 829.
[43] T. Miyazaki, Y. Koinuma, US Patent 5,936,703A (1999).
[44] Y.Z. Qiu, D.Y. Min, C. Ben, J. Shen, Q. Chen, S.C. Lin, Chin. J. Polym. Sci. 23 (2005) 611.
[45] L.N. Lewis, J. Stein, Y. Gao, R.E. Colborn, G. Hutchins, Platinum Met. Rev. 41 (1997) 66.
[46] S.J. Wang, X.D. Fan, J. Kong, J.R. Lu, Polymer 50 (2009) 3587.
[47] J. Wu, J.F. Antaki, W.R. Wagner, T.A. Snyder, B.E. Paden, H.S. Borovetz, ASAIO J. 51 (2005) 636.
[48] M.T. Bernards, G. Cheng, Z. Zhang, S. Chen, S. Jiang, Macromolecules 41 (2008) 4216.
[49] Z. Zhang, T. Chao, T. Chen, S. Jiang, Langmuir 22 (2006) 10072.

Characterization of the spatial immobilization manner of poly(ethylene glycol) to a titanium surface with immersion and electrodeposition and its effects on platelet adhesion

Yuta Tanaka,[1] Yuh Matsuo,[2] Takayuki Komiya,[1] Yusuke Tsutsumi,[1] Hisashi Doi,[1] Takayuki Yoneyama,[3] Takao Hanawa[1]

[1]*Department of Metals, Institute of Biomaterials and Bioengineering, Tokyo Medical and Dental University, Tokyo 101-0062, Japan*

[2]*Department of Materials Science, Shibaura Institute of Technology, Tokyo 135-8548, Japan*

[3]*Department of Dental Materials, Nihon University School of Dentistry, Tokyo 101-8310, Japan*

Received 26 May 2008; revised 7 October 2008; accepted 30 October 2008
Published online 2 February 2009 in Wiley InterScience (www.interscience.wiley.com). DOI: 10.1002/jbm.a.32375

Abstract: Both terminals of a poly(ethylene glycol) (PEG) molecule were terminated with amines. The PEG was electrodeposited onto titanium (Ti) to give it the biofunctions such as blood compatibility. The effects of the amine of PEG terminals and the pH at PEG solution on the adsorption amount of PEG molecules and the thickness of PEG layer immobilized on the Ti surface were evaluated using quartz crystal microbalance technique and X-ray photoelectron spectroscopy. The interfacial reactivity between PEG terminals and the Ti surface was the largest at pH 11, according to the interaction between the charge of terminal amines of PEG and the point of zero charge of Ti oxide. The orientations of PEG molecules immobilized on the Ti surface with immersion or electrodeposition at pH 11 were determined by Fourier transform infrared reflection absorption spectroscopy. Consequently, the terminal amines of PEG were oriented perpendicularly to the surface in electrodeposition rather than in immersion. The charged PEG randomly immobilized on the Ti surface with immersion led to platelet aggregation, whereas U-shaped PEG molecule immobilized with electrodeposition inhibited platelet adhesion and aggregation. The immobilization manners of PEG on the Ti surface were strongly associated with a biofunction such as platelet adhesion. © 2009 Wiley Periodicals, Inc. J Biomed Mater Res 92A: 350–358, 2010

Key words: titanium; poly(ethylene glycol); electrodeposition; surface analysis; blood compatibility

INTRODUCTION

Biofunctions, such as the inhibition of protein adsorption and cell adhesion to an artificial material surface, are required in the design of biomedical and bioanalytical devices. When metallic stents are placed in stenotic blood vessels for dilatation, blood compatibility on the metal surface is necessary. In guide wires and guiding catheters, sliding lubrication in blood vessels in addition to blood compatibility is important when the catheters are inserted. If metals are used as a biosensing device, cell adhesion must be controlled. However, no stage of the manufacturing process of metals, such as melting, casting, forging, and heat treatment, allows them to have these biofunctions. Therefore, biofunctions on a metal surface must be achieved by surface treatments or surface modifications.

Recently, the immobilization of functional molecules or biomolecules on metal surfaces is popular to create biofunctional metal surfaces.[1,2] Immobilization of poly(ethylene glycol) (PEG) on material surfaces is a preferred strategy for inhibiting protein adsorption.[3,4] Among the methods reported on the immobilization of PEG to metal surfaces, graft copolymers of poly(L-lysine) and poly(ethylene glycol) (PLL-*g*-PEG) have proven to be particularly attractive for rendering metal surfaces highly resistant to nonspecific protein adsorption following cell spreading and bacterial adhesion.[5–7] However, this method includes multistage processes for the synthesis of PLL-*g*-PEG and immobilization. In addition, the bonding between the PLL-*g*-PEG layer immobilized with immersion and metal oxides is considered to be weak. Therefore, we attempted to immobilize PEG on titanium (Ti) with electrodeposition, which is considered to be a simple and universal method for all metals.

Correspondence to: H. Doi; e-mail: doi.met@tmd.ac.jp

Previous studies reported that PEG terminated with amines at both terminals (NH_2-PEG-NH_2) inhibited protein absorption when immobilized on a Ti surface with electrodeposition.[8] In addition, the location of amines in the NH_2-PEG-NH_2 layer and the bonding state at the NH_2-PEG-NH_2/TiO_2 interface were characterized by X-ray photoelectron spectroscopy (XPS) and glow-discharge optical emission spectroscopy.[9] In the first layer of NH_2-PEG-NH_2 immobilized with electrodeposition, more terminated amines existed at the NH_2-PEG-NH_2/TiO_2 interface and combined with TiO_2 as a NHO bond formed between NH_3^+ and O^-. On the other hand, more amines randomly existed as a NH_3^+ bond in the NH_2-PEG-NH_2 layer immobilized with immersion. However, it remains unclear which condition is effective for accelerating the interfacial reactivity and whether or not the different spatial immobilization manners in immersion and electrodeposition influence their biofunctions.

A more suitable technique for spatial studies of immobilized molecules on metal surfaces is Fourier transform infrared reflection absorption spectroscopy (FTIR-RAS). The RAS in combination with the FTIR has been proven to be useful for the structural characterization of biomolecules immobilized on metal surfaces.[10,11] The RAS technique provides information not only about functional groups but also about the orientation of the immobilized molecules, because the infrared radiation interacts only with oscillating dipoles perpendicular to the surface. The adsorption orientations of proteins or amino acids on a metal surface have been investigated using FTIR-RAS.[5] In this study, the spatial configuration of NH_2-PEG-NH_2 immobilized on a Ti surface with immersion or electrodeposition was characterized with FTIR-RAS. In addition, the relationship between the spatial configuration and platelet adhesion was investigated.

MATERIALS AND METHODS

Specimen preparation

A commercially pure Ti disk (8 mm on diameter × 2 mm in thickness) with grade 2 (Rare Metallic Co., Japan) was mirror-polished with SiC paper, a 9 μm-diamond suspension, and a 0.04 μm-colloidal silica suspension. The disks were cleaned from macroscopic contamination by ultrasonication in acetone for 15 min, dried with a stream of nitrogen (99.9%), and stored in a desiccator until the immobilization of PEG. The sputter-deposited Ti on silicon (Si) wafers (Ti/Si) with a thickness of 100 nm using a sputter-deposition machine (ANELVA, Canon, Japan) were used for FTIR-RAS because an accurate spectrum on smooth and clean surfaces is necessary for the structural characterization of PEG molecules.

Immobilization of PEG to titanium with immersion and electrodeposition

We have employed a characteristic PEG molecule in which both terminals of PEG were terminated with NH_2 (NH_2-PEG-NH_2, PEG1000 Diamine, NOF Corporation, Japan). NH_2-PEG-NH_2 was dissolved in deionized water (Millipore) at a concentration of 2mass%, and the pH of the solution was adjusted to 8, 9, 10, and 11 by dropping 1 mol L^{-1} HCl. The original PEG without termination (Unmodified-PEG, NOF Corporation, Japan) was used for comparison with the quartz crystal microbalance (QCM) technique. The unmodified-PEG was dissolved in deionized water at a concentration of 2mass%, and the pH of the solution was adjusted to 3 and 11. The Ti was immersed in NH_2-PEG-NH_2 solutions adjusted to each pH at 310 K for 24 h. An NH_2-PEG-NH_2 solution with pH 11 was employed as electrolyte for electrodeposition because the interfacial reactivity was the largest in immersion. Electrodeposition was performed according to previous studies.[8,9] During cathodic polarization, NH_2-PEG-NH_2 migrated to the cathode (Ti or Ti/Si), where they were immobilized, as shown in Figure 1. Ti and Ti/Si surfaces are always covered with a passive oxide film, whose point of zero charge (PZC) is similar to that of the bulk TiO_2 surface.[12] After immersion and electrodeposition, each specimen was rinsed in deionized water and dried in flowing nitrogen (99.9%).

Monitoring of PEG adsorption to titanium with QCM

The adsorption of NH_2-PEG-NH_2 and unmodified-PEG to a Ti surface was monitored using a QCM technique. QCM is a mass-sensitive piezoelectric device capable of detecting small changes in the electrode mass in the region

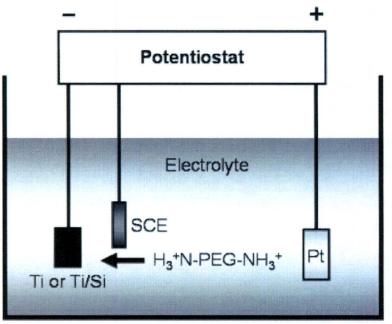

Figure 1. Schematic illustration of electrodeposition. During cathodic polarization, NH_2-PEG-NH_2 migrated to the cathode (Ti or Ti/Si), where it was immobilized. A 2mass% NH_2-PEG-NH_2 solution with a 0.3 mol L^{-1} NaCl solution was used as an electrolyte.

of 10 μg m^{-2}. A QCM electrode (quartz crystal of the A-T cut type, Hokuto Denko, Japan) with a fundamental resonant frequency of 6 MHz was sputter-deposited with Ti. The exposed area of Ti to the solution was 1.33 cm^2. When the crystal is made to oscillate at its resonant frequency, the fundamental frequency changes as mass is adsorbed on or desorbed from the electrode. The frequency shift (Δf) was monitored by an electrochemical QCM controller (model HQ101B, Hokuto Denko, Japan) connected to an electrochemical analysis system (model HZ-3000, Hokuto Denko, Japan). Platinum was used as the counter electrode, and a saturated calomel electrode (SCE) as the reference electrode. The Δf of the crystal was stabilized in deionized water for 1 h before injection of PEG solution. After 1 h, each PEG solution was injected with a syringe at a resultant concentration of 2mass%. The Δf of the crystal at 310 K was monitored for 24 h. Whole PEG molecules adsorbed on Ti surface were detected by QCM.

Thickness of the PEG layer determined by ellipsometry

On the other hand, the thicknesses of the residual NH_2-PEG-NH_2 layer on Ti after rinsing in deionized water were determined with an ellipsometry (DVA-36Ls, Mizojiri Optical Co., Japan) in air, and the detail is described somewhere.[8,9]

Interfacial bonding states determined by XPS

The chemical bonding states existing in the PEG layer immobilized with immersion at each pH were characterized using XPS (SSX100, Surface Science Instrument, USA). All binding energies given in this article are relative to the Fermi level, and all spectra were excited with the monochromatized Al Kα line (1486.61 eV). The spectrometer was calibrated against Au $4f_{7/2}$ (84.07 eV) and Au $4f_{5/2}$ (87.74 eV) of pure gold and Cu $2p_{3/2}$ (932.53 eV), Cu $2p_{1/2}$ (952.35 eV), and a Cu Auger $L_3M_{4,5}M_{4,5}$ line (918.65 eV) of pure copper. The energy values were based on published data.[13] The take-off angle for photoelectron detection was 35° from the surface of the specimen. To estimate the photoelectron peak intensities, the background was subtracted from the measured spectrum according to Shirley's method.[14]

Orientation of PEG molecules determined by FTIR-RAS

The FTIR-RAS was performed with an FTIR Spectrometer (JASCO, FT/IR-300, Japan). A liquid-nitrogen-cooled mercury cadmium telluride (MCT) detector was used to collect spectra with a resolution of 2 cm^{-1}. Figure 2 shows the mirror arrangement for the RAS. The angle of incidence was 85° to the surface normal. A polarizer was used to remove the perpendicular part of the infrared radiation. An untreated Ti/Si wafer was used as the reference. For both PEG-immobilized specimens and reference ones, spectra with 500 scans were collected. The resultant spectra for the discussion were obtained by subtracting those of the reference. The diffuse reflection spectrum of pure NH_2-PEG-NH_2 mixed with powdered potassium bromide (KBr) was obtained with 20 scans without RAS for comparison.

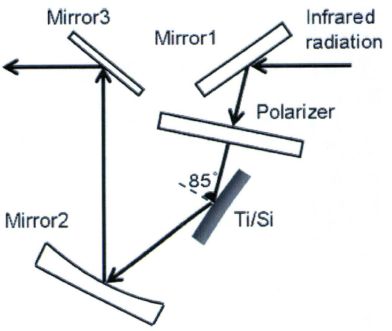

Figure 2. Mirror arrangement used for the RAS. The angle of incidence was 85° relative to the surface normal. The polarizer was used to remove the perpendicular part of the infrared radiation.

In vitro platelet adhesion experiment

Human blood from a healthy volunteer was drawn into a syringe with 1 mL of 3.8% sodium citrate solution used as an anticoagulant at a ratio of 9 parts blood to 1 part citrate. This study was approved by the Research Ethics Committee in the Institute of Biomaterials and Bioengineering, Tokyo Medical and Dental University before start. A total of 1×10^5 platelets μL^{-1} plate-rich plasma (PRP) was obtained from a freshly citrated blood. A 0.25 mol L^{-1} $CaCl_2$ solution was added to PRP. The untreated-Ti and electrodeposited-Ti, which were incubated at 310 K in advance, were immersed into PRP at 310 K for 5 min. Thereafter, they were rinsed with PBS(−), fixed with 2% glutaraldehyde, dehydrated, and observed through a scanning electron microscope, SEM (S-3400NX, Hitachi, Japan).

Statistical analysis

A statistical comparison was made using the one-way factorial ANOVA including the interaction effect and *post hoc* Tukey multiple comparison testing.

RESULTS AND DISCUSSION

Effect of charges of PEG terminals on the amount of physically adsorbed PEG

Figure 3 shows the time transient of a frequency shift monitored using QCM after the injection of

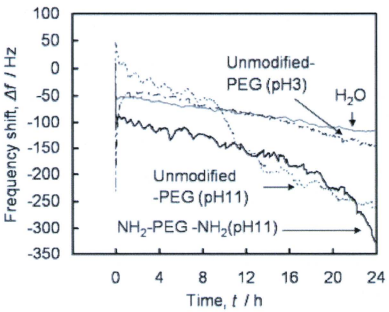

Figure 3. Time transient of the frequency shift after the injection of each PEG solution measured by QCM. The decreasing frequency shift indicates the increase of PEG molecules adsorbed on the Ti surface.

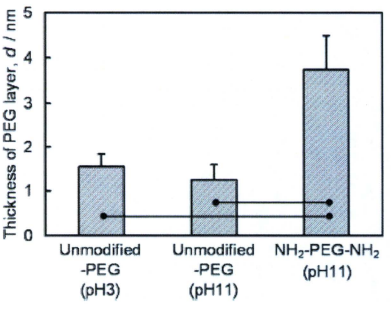

Figure 4. Thickness of the PEG layer on a Ti surface determined with ellipsometry, which leads to only chemically adsorbed PEG. The bars represent statistically significant differences ($p < 0.01$).

each PEG solution. The changes in the number of PEG molecules per unit area can be calculated from the frequency shift, and the decreasing frequency shift represents the increase of PEG molecules adsorbed on the Ti surface. Just after the injection, the mass on the Ti surface abruptly increased, followed by the immediate decrease of the mass. After 24 h from the injection, the mass at pH 11 was larger than that at pH 3. In the case of NH_2-PEG-NH_2 at pH 11, the mass gain after the injection was always much larger than that of unmodified-PEG at pH 3. The adsorption amount of NH_2-PEG-NH_2 after 24 h was equivalent to about 4.1 μg cm^{-2} (25 molecules nm^{-2}) according to the Sauerbrey expression.[15] This value means that the NH_2-PEG-NH_2 molecules formed a multilayer considering the number of hydroxyl groups (about 10 nm^{-2}) of the Ti oxide film. On the other hand, the mass at pH 3 was slightly larger than that of H_2O; the adsorbed amount of PEG itself was quite low. These results are supported by the PZC for TiO_2; the Ti surface was positively charged as Ti^+ at pH lower than pH 6.7, which is the PZC for anatase TiO_2, whereas it was negatively charged as O^- at higher pH. In other words, the negatively charged surface is susceptible to attract PEG molecules rather than a positively charged one. In addition, the mass of both NH_2-PEG-NH_2 and unmodified-PEG at pH 11 was almost the same. Therefore, the amount of physically adsorbed PEG on Ti is predominantly governed by the PZC of the surface oxide rather than the charges of the terminals. The adsorption amount was governed by the relative permittivity for each metal oxide in addition to the PZC when the different metals were compared.[16]

Effect of pH and terminals of PEG on the thickness of the chemically absorbed layer

Figure 4 shows the thickness of the PEG layer that remained on the Ti, which was measured using ellipsometry. In general, the thickness measured using ellipsometry increases with the increase of the adsorbed mass or density. The thickness in NH_2-PEG-NH_2 was significantly larger than that in unmodified-PEG because terminated amines charged as NH_3^+ and bonded chemically with negatively charged TiO_2 (O^-). This result agrees with the QCM results. On the other hand, the thickness in unmodified-PEG at pH 11 was almost the same as that at

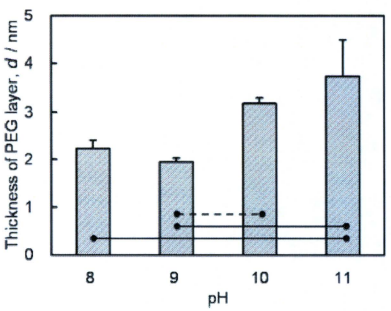

Figure 5. Thickness of the PEG layer absorbed from the NH_2-PEG-NH_2 solution at pH 8, 9, 10, and 11 determined with ellipsometry. The bars represent statistically significant differences; solid line, $p < 0.01$ and dashed line, $p < 0.05$.

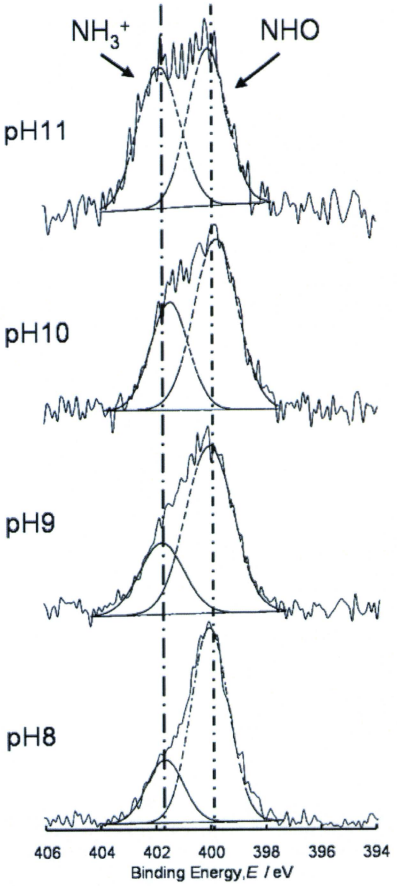

Figure 6. The XPS spectrum of the N 1s electron binding energy region consists of two peaks originating from a NH_3^+ bond and a NHO bond. The ratio of the integrated intensity of the NH_3^+ bond to the NHO bond increased with the increase of pH.

pH 3. This result is attributed to the desorption of unmodified-PEG; most of unmodified-PEG molecules physically adsorbed at pH 11 and desorbed during rinsing because unmodified-PEG does not have a charge. The thickness of the NH_2-PEG-NH_2

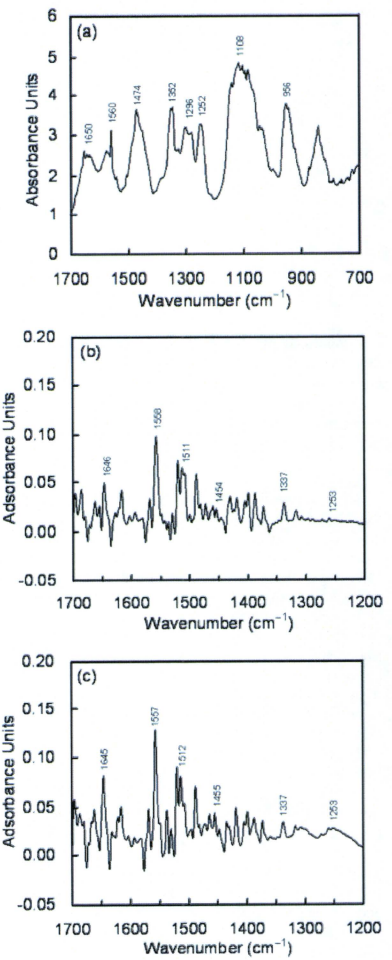

Figure 7. (a) FTIR spectrum of NH_2-PEG-NH_2 powder (in a pressed KBr tablet). (b) FTIR-RAS spectrum of NH_2-PEG-NH_2 immobilized with immersion on a Ti surface. (c) FTIR-RAS spectrum of NH_2-PEG-NH_2 immobilized with electrodeposition on a Ti surface.

TABLE I
Vibrational Band Frequencies and Assignments

Mode Assignment	NH_2-PEG-NH_2 (KBr)	Immersed NH_2-PEG-NH_2	Electrodeposited NH_2-PEG-NH_2
N—H bending	1650	1646	1645
C—N stretching	1560	1558	1557
N—H scissoring	–	1511	1512
C—H scissoring	1474	1454	1455
C—H wagging	1352	1337	1337
C—H twisting	1296	–	–
C—H twisting	1252	1253	1253
C—O, C—C stretching	1108	–	–
C—H rocking	956	–	–

chemisorbed layer is in a higher pH range than the PZC, pH 8, 9, 10, and 11, is shown in Figure 5. The thicknesses at pH 10 and 11 were significantly larger than those at other pH values because the surface at higher pH has a higher proportion of negatively charged hydroxyl groups (O^-). The reactivity between TiO_2 and PEG molecules was the largest at pH 11 in immersion.

The pH-dependent interfacial bonding between TiO_2 and PEG

The bonding at the interface between TiO_2 and PEG molecules was evaluated by the XPS spectra of an N 1s electron energy region. The XPS spectrum of the N 1s electron binding energy region consists of two peaks originating from the NH_3^+ bond and the NHO bond, as shown in Figure 6.[17,18] The NH_3^+ bond detected by XPS is considered to be weaker than the NHO bond. In fact, more NH_3^+ bonds at the interface existed in immersion than in electrodeposition.[8,9] The ratio of the integrated intensity of the NH_3^+ bond to the NHO bond increased with the increase of the pH. Therefore, the thickness of the NH_2-PEG-NH_2 layer at pH 11 was the largest, while more NH_3^+ weak bond existed at the interface rather than other pHs. As a result, the NH_2-PEG-NH_2 solution adjusted at pH 11 was employed for electrodeposition in this study. In previous studies, it was shown that a NHO bond is efficiently formed by 300-s electrodeposition rather than 24-h immersion at pH 11.[8]

Orientation of PEG molecules electrodeposited on a titanium surface

Reflection-absorption infrared spectroscopy has been thoroughly studied to investigate the orientation of the molecules immobilized on a metallic surface. Only the component of the vibrational transition dipole moments perpendicular to the surface plane contributes to the absorbance spectra. Therefore, this technique provides information not only on functional groups but also on the orientation and conformation of adsorbed molecules or molecular entities. The IR spectrum of pure NH_2-PEG-NH_2 powder (in a KBr tablet) was measured first as a control to discuss the vibrational spectra of NH_2-PEG-NH_2, as shown in Figure 7(a). The RAS spectrum of the NH_2-PEG-NH_2 immobilized on Ti with immersion or electrodeposition is shown in Figure 7(b,c). The vibrational band frequencies and assignments are listed in Table I. The absorbance at 1557 cm^{-1}, which is ascribed to the C—N stretching mode, in electrodeposition was 1.3 times stronger

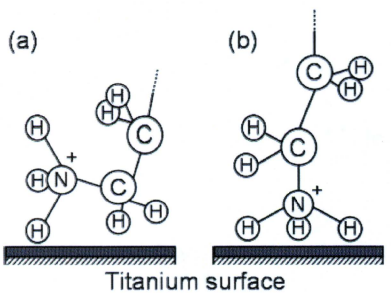

Figure 8. Suggested orientation model of NH_2-PEG-NH_2 molecules to a Ti surface; (a) immersion, (b) electrodeposition. The terminals of NH_2-PEG-NH_2 molecules were oriented perpendicular to a Ti surface and formed a U-shape in the case of electrodeposition; the NH_2-PEG-NH_2 molecules were randomly immobilized on a Ti surface in the case of immersion.

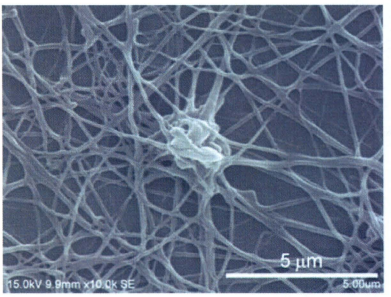

Figure 9. Ca^{2+}-activated platelet spread on the surface.

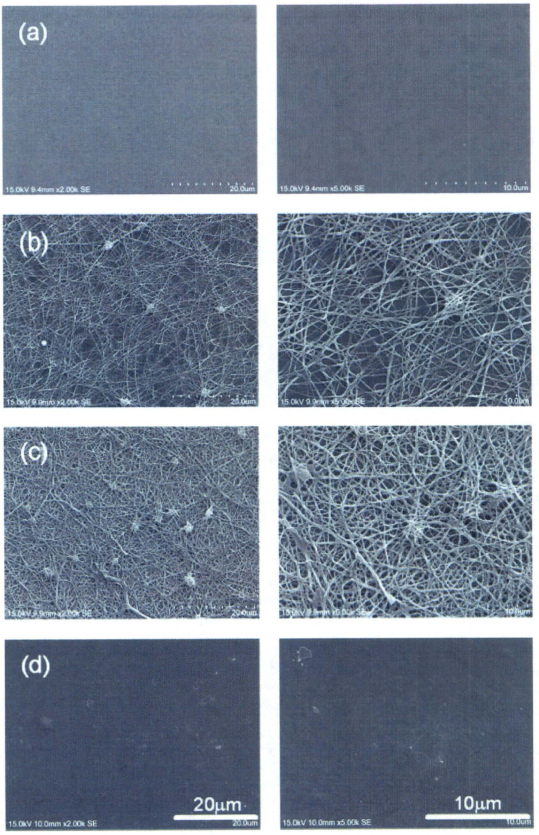

Figure 10. (a) SEM images of Ti surface before exposure to PRP, (b) adherent platelets spread on Ti, (c) NH_2-PEG-NH_2-immobilized Tiwith immersion, and (d) NH_2-PEG-NH_2-immobilized Tiwith electrodeposition.

than that in immersion. Because only the component of the vibrational transition dipole moments perpendicular to the surface contributes to the adsorption spectra, the C—N bonding of the NH_2-PEG-NH_2 terminals in electrodeposition was considered to be oriented perpendicular to the Ti surface rather than in immersion. Moreover, the ratio of N—H scissoring mode at 1512 cm^{-1} to CH_2 scissoring mode at 1455 cm^{-1} in electrodeposition (1.9) was smaller than that in immersion (2.9). Contrary to the stretching mode, the vibrational transition dipole moments parallel to the surface contributes to the adsorption spectra. Therefore, the N—H bond of the NH_2-PEG-NH_2 terminals in electrodeposition was considered to be oriented perpendicular to the Ti surface rather than in immersion. Therefore, the orientation model to the Ti surface was suggested, as shown in Figure 8. The terminals of NH_2-PEG-NH_2 molecules were oriented perpendicular to the Ti surface and formed U-shape immobilization in the case of electrodeposition; the

NH_2-PEG-NH_2 molecules were randomly immobilized on a Ti surface in the case of immersion. In the case of electrodeposition, some layers of NH_2-PEG-NH_2 will be formed on the first layer. Of course, U-shape was not formed over second layers.

In vitro platelet adhesion

Platelet adhesion was evaluated as a parameter for the blood compatibility of specimens in separating platelets from other blood components. Platelet activation is a controlled sequence of actin filament serving, uncapping, elongation, recapping, and crosslinking that creates a dramatic shape change in the platelet. Ca^{2+}-activated platelets spread on the surface as shown in Figure 9; platelet aggregation is caused by fibrinogen. An image of Ti surface before exposure to PRP is shown in Figure 10(a). Figure 10(b–d) shows the SEM images of adherent platelets spread on NH_2-PEG-NH_2-immobilized Ti by immersion or electrodeposition and untreated Ti. Fewer platelets adhered on electrodeposited Ti than immersed and untreated Ti. This result indicated that platelet adhesion was inhibited by electrodeposited PEG molecules on Ti because they are not exposed to the charges of amines on the surface for the NHO bond of the interface. In addition, the platelet aggregation was inhibited by the protein adsorption resistance of PEG itself. If the surface is positively charged as NH_3^+, the zwitterionic proteins are attracted to the charged surface regardless of the effect of PEG itself. In the case of immersion, the platelet adhesion and aggregation were caused by the charged amines of NH_2-PEG-NH_2 adsorbed on the Ti surface, as shown in Figure 10(c). Also, the adsorbed PEGs in immersion may desorb and result in the platelet aggregation because their interfacial bond with TiO_2 is weak. It is important to control the immobilization manners of biofunctional molecules, including the surface charges by surface treatments or surface modification. As a result, electrodeposition is useful for controlling the orientation and immobilization amount of PEG molecules.

CONCLUSIONS

The results using QCM and an ellipsometry demonstrated that the thickness of the NH_2-PEG-NH_2 layer at pH 11 was the largest. The NH_2-PEG-NH_2 solution adjusted at pH 11 was employed for electrodeposition, and the orientation of electrodeposited NH_2-PEG-NH_2 molecules was investigated using the FTIR-RAS technique. As a result, the terminal amines of PEG were oriented perpendicularly to the Ti surface in electrodeposition rather than in immersion. These results indicated that the PEG molecules were immobilized perpendicularly on the Ti surface and formed a U-shaped immobilization in the case of electrodeposition; they were randomly immobilized on a Ti surface in the case of immersion. The PEG molecules immobilized in a U-shape on a Ti surface inhibited platelet adhesion and aggregation, whereas randomly immobilized PEG molecules formed platelet aggregation. The immobilization manners of PEG on a Ti surface are attributed to a biofunction, such as the inhibition of platelet adhesion.

The authors thank Drs. Kimura and Ohtsu of the Institute for Materials Research, Tohoku University, for their assistance in the measurement of XPS. This study was performed under the inter-university cooperative research program of the Laboratory for the Department of Biomaterials Science, Institute for Materials Research, Tohoku University.

References

1. Schuler M, Owen GR, Hamilton DW, Wild M, Textor M, Brunette DM, Tosatti SGP. Biomimetic modification of titanium dental implant model surface using the RGDSP-peptide sequence: A cell morphology study. Biomaterials 2006;27: 4003–4015.
2. Rezania A, Johnson R, Lefkow AR, Healy KE. Bioactivation of metal oxide surface. I. Surface characterization and cell response. Langmuir 1999;15:6931–6939.
3. Hansson KM, Tosatti S, Isaksson J, Wettero J, Textor M, Lindahl TL, Tengvall P. Whole blood coagulation on protein adsorption-resistant PEG and peptide functionalized PEG-coated titanium surface. Biomaterials 2005;26:861–872.
4. Zhang F, Kang ET, Neoh KG, Wang P, Tan KL. Surface modification of stainless steel by grafting of poly(ethylene glycol) for reduction in protein adsorption. Biomaterials 2001;22: 1541–1548.
5. Huang NP, Michel R, Voros J, Textor M, Hofer R, Rossi A, Elbert DL, Hubbell JA, Spencer ND. Poly(L-lysine)-g-poly(ethylene glycol) layers on metal oxide surface: Surface-analytical characterization and resistance to serum and fibrinogen adsorption. Langmuir 2001;17:489–498.
6. Tosatti S, Paul SM, Askendal A, VandeVondele S, Hubbell JA, Tengvall P, Textor M. Peptide functionalized poly(L-lysine)-g-poly(ethylene glycol) on titanium: Resistance to protein adsorption in full heparinized human blood plasma. Biomaterials 2003;24:4949–4958.
7. Harris LG, Tosatti S, Wieland M, Textor M, Richards RG. *Staphylococcus aureus* adhesion to titanium oxide surface coated with non-functionalized and peptide-functionalized poly(L-lysine)-grafted-poly(ethylene glycol) copolymers. Biomaterials 2004;25:4135–4148.
8. Tanaka Y, Doi H, Iwasaki Y, Hiromoto S, Yoneyama T, Asami K, Imai H, Hanawa T. Electrodeposition of amine-terminated poly(ethylene glycol) to titanium surface. Mater Sci Eng C 2007;27:206–212.
9. Tanaka Y, Doi H, Kobayashi E, Yoneyama T, Hanawa T. Determination of immobilization manner of amine-terminated poly(ethylene glycol) electrodeposited to titanium surface with XPS and GD-OES. Mater Trans 2007;48:287–292.
10. Liedberg B, Ivarsson B, Lundstrom I, Salaneck WR. Fourier transform infrared reflection absorption spectroscopy (FT-IRAS) of some biologically important molecules absorbed on metal surfaces. Prog Colloid Polym Sci 1985;70:67–75.

11. Liedberg B, Ivarsson B, Lundstrom I. Fourier transform infrared reflection absorption spectroscopy (FT-IRAS) of fibrinogen absorbed on metal and metal oxide surface. J Biochem Biophys Meth 1984;9:233–243.
12. Kurrat R, Walivaara B, Marti A, Textor M, Tengvall P, Ramsden JJ, Spencer ND. Plasma protein adsorption on titanium: Comparative *in situ* studies using optical waveguide lightmode spectroscopy and ellipsometry. Colloids Surf B: Biointerface 1998;11:187–201.
13. Asami K. A precisely consistent energy calibration method for X-ray photoelectron spectroscopy. J Electron Spectrosc 1976;9:469–478.
14. Shirley DA. High-resolution X-ray photoemission spectrum of the valence bands of gold. Phys Rev B 1972;5:4709–4714.
15. Sauerbrey GZ. Verwendung von Schwingquarzen zur Wägung dünner Schichten und zur Mikrowägung. Z Phys 1959;155:206–222.
16. Tanaka Y, Saito H, Tsutsumi Y, Doi H, Imai H, Hanawa T. Active hydroxyl groups on surface oxide film of titanium, 316L stainless steel, and cobalt-chromium-molybdenum alloy and its effect on the immobilization of poly(ethylene glycol). Mater Trans 2008;49:805–811.
17. Losito I, Malitesta C, Bari ID, Calvano C. X-ray photoelectron spectroscopy characterization of poly(2,3-diaminophenazine) films electrosynthesized on platinum. Thin Solid Films 2005;473:104–113.
18. Sousa SR, Moradas-Ferreira P, Barbosa MA. TiO_2 type influences fibronectin adsorption. J Mater Sci: Mater Med 2005;16:1173–1178.

Differences in the bone differentiation properties of MC3T3-E1 cells on polished bulk and sputter-deposited titanium specimens

Kei Oya,[1] Yuta Tanaka,[1] Yoshihisa Moriyama,[2] Yuki Yoshioka,[3] Tsuyoshi Kimura,[1] Yusuke Tsutsumi,[1] Hisashi Doi,[1] Naoyuki Nomura,[1] Kazuhiko Noda,[2] Akio Kishida,[1] Takao Hanawa[1]

[1]Institute of Biomaterials and Bioengineering, Tokyo Medical and Dental University, 2-3-10 Kanda-Surugadai, Chiyoda-ku, Tokyo 101-0062, Japan

[2]Department of Materials Science and Engineering, Shibaura Institute of Technology, 3-7-5 Toyosu, Koto-ku, Tokyo 135-8548, Japan

[3]Faculty of Dentistry, Tokyo Medical and Dental University, 1-5-45 Yushima, Bunkyo-ku, Tokyo 113-8510, Japan

Received 29 May 2009; revised 28 October 2009; accepted 11 November 2009
Published online 2 March 2010 in Wiley InterScience (www.interscience.wiley.com). DOI: 10.1002/jbm.a.32751

Abstract: The roughness and cleanness of a titanium surface must be controlled in order to investigate the expression mechanism of hard tissue compatibility on titanium. In this study, osteogenic MC3T3-E1 cells were cultured and differentiation-induced on bulk and sputter-deposited titanium specimens, and the osteogenesis were investigated. For the preparation of bulk specimens, titanium discs were mirror-polished. On the other hand, titanium was sputter-deposited on smooth and clean cover glasses as sputter-deposited specimens. As a result, no significant difference was observed in the cell morphology and attached number. On the other hand, the time showing maximum activity in the alkaline phosphatase and gene expressions, which are related to bone differentiation on the bulk titanium, were superior to those on the sputter-deposited titanium. From the surface observation of the specimens with a scanning electron microscope and a scanning probe microscope, the surface on the sputter-deposited titanium was more uniform and cleaner than that on the bulk titanium. According to X-ray photoelectron spectroscopy, the thickness of surface oxide film on the sputter-deposited titanium was smaller than that on the bulk titanium. In addition, the proportions of TiO and Ti_2O_3 in the surface oxide film on the sputter-deposited titanium were larger than those on the bulk titanium. These differences might influence the differentiation of osteoblastic cells. © 2010 Wiley Periodicals, Inc. J Biomed Mater Res Part A: 94A: 611–618, 2010

Key Words: titanium, bulk bodies, sputter deposition, MC3T3-E1 cells, bone differentiation properties

INTRODUCTION

Metals are widely used as biomaterials because of their excellent strength and toughness. Titanium and its alloys are applied for dental and orthopedic devices because they show good corrosion resistance and hard tissue compatibility among metals. However, the mechanism of the good hard tissue compatibility of titanium has not been completely elucidated. Therefore, the elucidation of the mechanism is necessary. For this purpose, the surface roughness and cleanness must be controlled.

For elucidating the expression mechanism of the good hard tissue compatibility, it is important to first observe the differentiation of osteoblast on titanium. The cell culture test using a cell line *in vitro* has some advantages as follows: (1) The design of experimental procedure is easier than *in vivo* test, and (2) the results are not affected by any other factors in the exception of the designed conditions. On the other hand, bulk titanium bodies are usually employed in most researches about the hard tissue compatibility of titanium. However, the use of them represents the following disadvantages in the cell culture evaluation: (1) Living cells adhered on bulk specimens cannot be directly observed by a phase-contrast microscope because they are opaque, (2) it is difficult to completely remove impurities remaining on the surfaces, such as abrasives remaining after polishing, and (3) it is also difficult to completely eliminate scratches from the surface even after mirror-polishing.

To overcome these problems, the sputter deposition of titanium on a transparent substrate, such as glass, is effective. It is a technique that can form a thin film on the substrate at an atomic level.[1] The principle of sputter deposition is as follows: A plasma discharge is generated by applying a voltage after decreasing the atmosphere pressure while setting up a target (a titanium disc in this case) at the cathode and a substrate at the anode. The positive argon ions produced in a glow discharge attack the target; subsequently, target atoms are sputtered, and the atoms are then physically adsorbed on the substrate. This process allows the formation of a thin metal film enough to be see-through because the thickness is controlled. Therefore, the living

Correspondence to: T. Hanawa; e-mail: hanawa.met@tmd.ac.jp